Chemical Science

ROYAL SOCIETY OF CHEMISTRY

EDGE ARTICLE

View Article Online
View Journal | View Issue

Cite this: *Chem. Sci.*, 2025, **16**, 1321

All publication charges for this article have been paid for by the Royal Society of Chemistry

Efficient encapsulation of insulin by a giant macrocycle as a powerful approach to the inhibition of its fibrillation†

Ruotong Wang,[a] Zihan Fang,[a] Shenghui Li,[a] Ziliang Zhang,[b] Ming Dong,[a] Junyi Chen,*[ab] Qingbin Meng *[b] and Chunju Li *[a]

Received 9th October 2024
Accepted 6th December 2024

DOI: 10.1039/d4sc06859a

rsc.li/chemical-science

Diabetes is a lifelong metabolic disease that requires frequent subcutaneous injections of insulin. However, free insulin is prone to forming immunogenic fibrillar aggregates under physiologic conditions, which limits its biomedical applications. Here, an approach to inhibiting insulin fibrils was developed through entire encapsulation by a giant macrocyclic inhibitor agent. Negatively charged water-soluble Pentaphen[3]arene sulfate (PP[3]AS), bearing 15 benzenes on its skeleton, was designed and synthesized. *In vitro* and *in vivo* safety tests preliminarily demonstrated that PP[3]AS had excellent biocompatibility. PP[3]AS could not only effectively inhibit the formation of amyloid, but also disaggregate intractable mature insulin fibrils. This macrocyclic inhibitor exhibited effective host–guest complexation toward insulin at the C-terminal 11-mer peptide sequence of the B chain with association constants of $(5.69 \pm 0.50) \times 10^6$ M^{-1}. Such complexation behavior is distinctive to traditional macrocycles, which can only recognize amino acid residues from the side due to their limited cavity sizes. Control experiments also proved that smaller cucurbit[7]uril and carboxylatopillar[5]arene could not prevent insulin from fibrillation under the same test conditions. Notably, co-administration with equimolar PP[3]AS maintained normoglycemia for at least 300 min in streptozotocin-induced diabetic model mice, whereas mice that received free insulin became hyperglycemic again within ~150 min.

Introduction

Diabetes, an insidious and chronic disease caused by insufficient insulin secretion by the pancreas or the failure of cells to respond to insulin, is one of the most pressing global healthcare challenges.[1,2] The incidence of all forms of diabetes is increasing, coupled with extensive suffering, comorbidities, and economic burdens. Subcutaneous injection of insulin, a 51-mer protein hormone composed of two chains linked by disulfide bonds, is currently among the most common clinical treatments.[3–5] Natural insulin mainly exhibits an α-helical structure, but it tends to form insoluble amyloid fibrils, resulting in a reduction in insulin potency.[6–8] In addition, the instability of insulin also makes the production, storage, and transportation rather difficult.[9,10] Therefore, there is a great need to inhibit insulin fibrillation.

For the past few years, various types of inhibitors have been discovered to arrest the formation of amyloid fibrils, such as small molecule compounds,[11,12] polymers,[13–15] peptides,[16,17] ionic liquids,[18] and co-assembly.[19] One core issue in inhibiting insulin fibrillation is molecular recognition.[20,21] Macrocyclic receptors with pre-organized cavities and multiple binding sites are potential receptors for insulin. However, the average diameters of traditional macrocycles such as cyclodextrins,[22] cucurbiturils,[23] calixarenes,[24] and pillararenes[25] are usually less than 1 nm. These macrocycles are well suited to small and medium volume guest molecules, but cannot encapsulate biological macromolecules.[26] For proteins, they can only recognize certain amino acid residues from the side, resulting in an unsatisfactory influence on proteins' structures and functions. It is quite an interesting approach to encapsulate a specific region of insulin with a giant macrocycle to inhibit its fibrillation.

It is challenging to synthesize stable macrocycles with large-sized cavities. It should be noted that an increase in monomer numbers would cause folding and twisting of the macrocycles, and could not afford large-sized cavities. Very recently, our group developed a modular strategy for macrocycles, referred to as extended biphen[*n*]arenes; the cavity sizes can be customized by controlling the length of the rigid monomers. According to

[a]*Academy of Interdisciplinary Studies on Intelligent Molecules, Tianjin Key Laboratory of Structure and Performance for Functional Molecules, College of Chemistry, Tianjin Normal University, Tianjin, 300387, P. R. China; Web: jychen_msc.yeah.net. E-mail: cjli@shu.edu.cn*

[b]*Department State Key Laboratory of National Security Specially Needed Medicines, Beijing Institute of Pharmacology and Toxicology, Beijing, 100850, P. R. China. E-mail: nankaimqb@sina.com*

† Electronic supplementary information (ESI) available: General materials and methods, synthesis procedure of PP[3]AS, supporting results and experimental raw data. See DOI: https://doi.org/10.1039/d4sc06859a

the structure of insulin, we hypothesized that the C-terminal 11-mer peptide sequence (GERGFFYTPKT) at the B chain with two positively charged amino acid residues (R and K) and three types of hydrophobic amino acid residues (F, Y, and P) could be successfully encapsulated by a negatively charged giant macrocycle.

With the aim of encapsulation of the C-terminal 11-mer peptide sequence, in the present work, we designed and synthesized an anionic water-soluble pentaphen[3]arene (PP[3]AS) containing 15 benzenes on its skeleton and electrostatic recognition sites of sulfate groups on its portals, which could not only effectively inhibit the formation of amyloid, but also disaggregate intractable mature insulin fibrils. The biocompatibility of PP[3]AS was carefully evaluated for safety in practical applications. In streptozotocin-induced diabetic model mice, an equimolar mixture of insulin and PP[3]AS could increase the insulin activity (Fig. 1). In particular, giant PP[3]AS could encapsulate insulin at specific peptide fragments, in stark contrast to traditional receptors which can only recognize amino acid residues from the side.

Results and discussion

Efficient insulin-encapsulating macrocycles should exhibit the following characteristics: (1) a clearly defined molecular structure to ensure lot-to-lot consistency; (2) strong and specific binding affinity to insulin; (3) excellent aqueous solubility and biological compatibility. Pentaphen[3]arenes, with their triangular-prism structure and ~25 Å-long pendant arms, were screened as macrocyclic scaffolds due to their large cavity, facial derivatization, and distinctive recognition properties. The introduction of multiple sulfate groups on both rims was designed to increase solubility and enhance recognition strength to insulin *via* electrostatic interactions. Fig. 2 shows the four-step synthetic procedure of pentaphen[3]arene sulfates (PP[3]AS). Briefly, the pentaphenyl monomer (PP-OMe), which was conveniently prepared from commercial reagent 4,4″-dibromo-terphenyl and 2,4-dimethoxyphenylboronic acid, could cyclize to deliver *per*-methoxy pentaphen[3]arene (PP[3]A-OMe) in the presence of paraformaldehyde and boron trifluoride etherate. The *per*-hydroxylated pentaphen[3]arene (PP[3]A-OH) was quantitatively prepared by the deprotection of PP[3]A-OMe using excess BBr_3. Subsequently, PP[3]A-OH reacted with pyridine sulfur trioxide in pyridine to deliver PP[3]AS in 69.3% yield. Detailed synthetic procedures and compound characterization are provided in the ESI (Fig. S1–S8†).

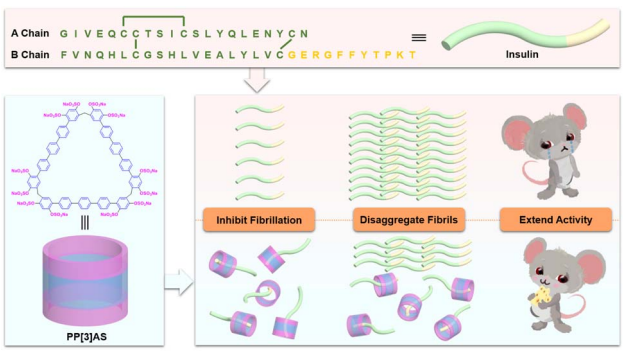

Fig. 1 The amino acid sequence of insulin and the molecular structure of PP[3]AS. An illustration of PP[3]AS inhibiting the fibrillation of insulin, disaggregating mature fibrils and extending activity in diabetic mice.

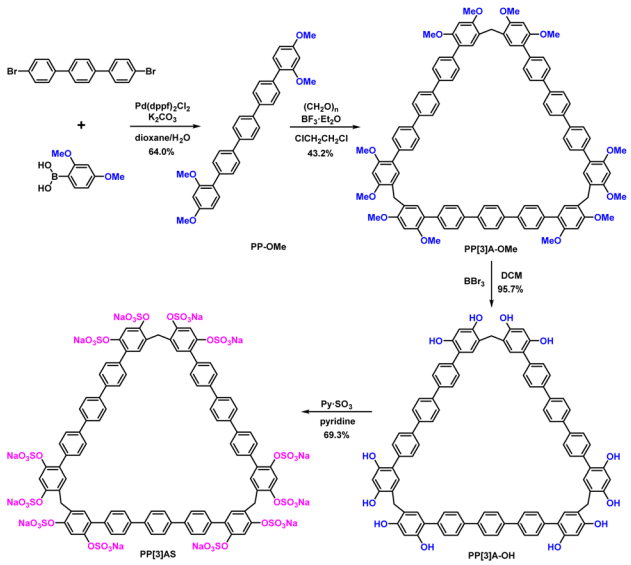

Fig. 2 The synthesis route to pentaphen[3]arene sulfates (PP[3]AS).

Using a fluorescent indicator displacement assay,[27–29] we first investigated the binding affinity between PP[3]AS and insulin. Rhodamine 123 (Rho123) was selected as the optimal reporter dye due to its high brightness and drastic complexation-induced quenching of fluorescence. The complexation stoichiometry of Rho123/PP[3]AS was determined to be 1 : 1 according to the continuous variation method result (Fig. S9†). Rho123 was strongly complexed by PP[3]AS with an association constant (K_a) of $(6.56 \pm 0.79) \times 10^6\ M^{-1}$, which is ideal for the projected competitive titrations (Fig. S10†). The displacement of Rho123/PP[3]AS by gradual addition of insulin resulted in the regeneration of the intrinsic emission of Rho123. Fitting the data by a 1 : 1 competitive binding model yielded a K_a value of $(5.69 \pm 0.50) \times 10^6\ M^{-1}$ (Fig. 3a and b). Host–guest complexation of insulin and PP[3]AS was further extrapolated by geometry optimization.[30] As shown in Fig. S11,† the energy-minimized model of insulin had dimensions of 2.05 × 1.71 × 6.18 nm, which well fitted to the cavity size of pentaphen[3]arene scaffold.[31] For the complex, PP[3]AS exhibited an entire encapsulation toward insulin, with a binding site of C-terminal 11-mer peptide sequence at the B chain (GERGFFYTPKT, P11) with a more favorable formation of heat (-7142.02 kcal mol^{-1}) (Fig. S12 and S13†). The central cyclic peptide region was hard to thread through the host, presumably as a consequence of a mismatch in molecular dimensions. To further verify the binding models, the binding affinity between PP[3]AS and P11 was also assessed using competitive titrations. Upon gradual addition of P11, the intrinsic emission of Rho123 was also regenerated, and the binding affinity of P11/PP[3]AS was

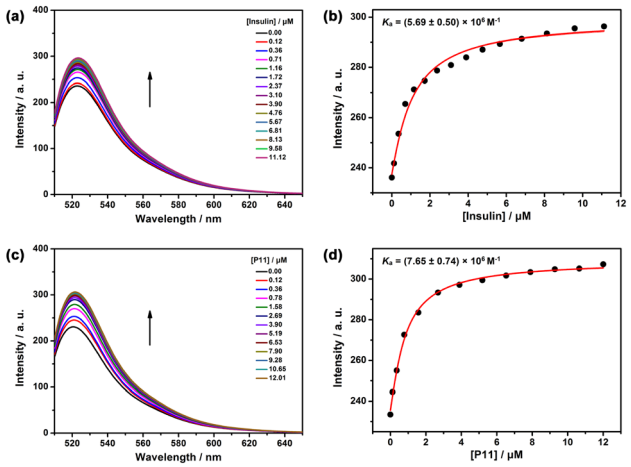

Fig. 3 (a) Competitive fluorescence titration of insulin in the presence of Rho123 (0.50 μM)/PP[3]AS (0.50 μM) in 10 mM PBS buffer at pH 7.4, λ_{ex} = 500 nm. (b) The associated competitive titration curve at λ_{em} = 525 nm and fit according to a 1 : 1 competitive binding model. (c) Competitive fluorescence titration of P11 in the presence of Rho123 (0.50 μM)/PP[3]AS (0.50 μM) in 10 mM PBS buffer at pH 7.4, λ_{ex} = 500 nm. (d) The associated competitive titration curve at λ_{em} = 525 nm and fit according to a 1 : 1 competitive binding model.

calculated to be (7.65 ± 0.74) × 10^6 M^{-1}, which was comparable to the K_a value of insulin/PP[3]AS (Fig. 3c and d). The N-terminal 5-mer peptide sequence (GIVEQ) at the A chain and N-terminal 6-mer peptide sequence (FVNQHL) at the B chain were also used to competitively titrate with Rho123/PP[3]AS, and no reasonable association constants could be obtained (Fig. S14 and S15†). Hence, the above findings led us to suggest that PP[3]AS recognized insulin *via* binding to the P11 sequence.

In addition, the control experiment demonstrated that smaller terphen[3]arene sulfates (TP[3]AS)[32] bearing 9 benzenes did not possess host–guest binding ability since no obvious fluorescence changes of Rho123 occurred upon addition of insulin (Fig. S16 and S17†). Furthermore, we measured the binding potency of lysine, arginine, phenylalanine, tyrosine and proline to PP[3]AS using the same competitive titration method (Fig. S18–S22†). Upon addition of these specific amino acids, no significant fluorescence regeneration of Rho123 was observed, indicating no complexation or at least relatively weak interactions. Previous studies have shown that traditional macrocycles, like cucurbiturils, calixarenes, pillararenes, and so forth, could bind terminal aromatic or basic amino acids. For giant PP[3]AS, failure of recognition was ascribed to unsatisfactory dimension matching. In other words, the capacity of PP[3]AS was sufficient for entirely encapsulating insulin at the P11 sequence, but it could not afford the binding to residues.

In view of the complicated physiological environment, it would be a prerequisite to selectively recognize the target rather than other ubiquitous biological macromolecules. To exclude the possibility of occupation of the endogenous interference within the cavity of PP[3]AS, we further tested the changes in the fluorescence intensity of Rho123/PP[3]AS caused by several important biological species, including lipase, trypsin, α-amalyse, *etc.* As shown in Fig. S23 in the ESI,† the addition of the above endogenous species caused no obvious fluorescence change, validating the excellent recognition selectivity of PP[3]AS towards insulin. Such robust binding affinities and excellent selectivity of PP[3]AS are beneficial for regulating the aggregation behavior of insulin.

Several methods can be used to characterize insulin aggregation, including fluorescence detection, turbidity, circular dichroism (CD), and transmission electron microscopy (TEM).[33] The existence of insoluble protein aggregates leads to an apparent increase in UV absorbance at all wavelengths due to the scattering effects.[34] To verify the above hypothesis, we first measured the absorbance at 540 nm to monitor the kinetics of insulin aggregation, where native insulin and PP[3]AS have negligible absorbance. As shown in Fig. 4a, the absorbance value of free insulin was increased over the course of 240 h, revealing that aggregation occurred in physiologic salt concentrations using 10 mM phosphate buffer saline (pH = 7.4). Noticeably, incubation of insulin with the equimolar PP[3]AS resulted in a sharp reduction in the absorbance signal at 540 nm. As mentioned above, traditional macrocycles are able to recognize specific amino acid residues in order to exert influence on an entire peptide or protein. Here two popular macrocycles, cucurbit[7]uril (CB[7])[35] and carboxylatopillar[5]arene (CP5A)[36] which could respectively bind to phenylalanine (for CB[7]), lysine, arginine and histidine (for CP5A) were chosen as control compounds. As shown in Fig. S24,† co-dosing with either CB[7] (3 eq.) or CP5A (4 eq.) displayed no obvious inhibition function on insulin fibrillation. These findings led us

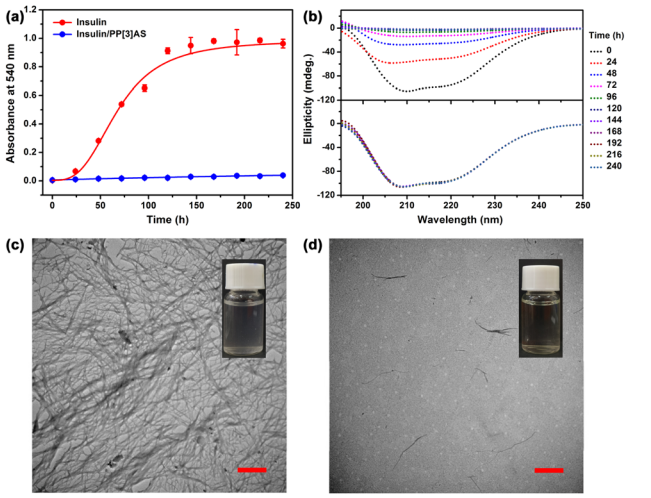

Fig. 4 (a) The kinetics of insulin (172 μM) aggregation in 10 mM PBS buffer at pH 7.4, monitored by an absorbance assay in the absence and presence of PP[3]AS (172 μM). Data are from n = 3 independent experiments and presented as mean ± SD. (b) Circular dichroism spectra of (top) free insulin (172 μM) and (bottom) insulin/PP[3]AS (172/172 μM) in 10 mM PBS buffer (pH = 7.4) at different time points. TEM images of (c) free insulin (172 μM) and (d) insulin/PP[3]AS (172/172 μM) in 10 mM PBS buffer aged for 144 h (scale bar = 1 μm). (Inset) photographs of insulin (172 μM) in the absence and presence of PP[3]AS (172 μM) in PBS buffer aged for 144 h.

to believe that entire complexation by a giant macrocycle has an evident advantage in dosage and efficacy against insulin fibrils.

CD spectra were then performed to analyze the effect of PP[3]AS on the secondary structure transition of insulin during the amyloid formation period. Previous studies have reported that native insulin possesses an α-helix confirmation with two negative bands at 208 nm and 222 nm.[37] As shown in Fig. 4b, the ellipticities at the above two wavelengths of free insulin increased progressively, which was ascribed to a fibration-induced concentration decrease in PBS solution. In comparison, the CD spectra of insulin/PP[3]AS remained almost unchanged over a period of 240 h. To further prove the inhibition properties of PP[3]AS, TEM was used to observe the ultramorphological changes. Insulin alone generated large amounts of mature fibrils (Fig. 4c), whereas in the presence of PP[3]AS, no trace of fibrils could be found (Fig. 4d). Taken together, these results revealed that complexation by PP[3]AS could efficiently inhibit the fibrillogenesis of insulin.

Although significant research has been dedicated to preventing the formation of insulin amyloid, disaggregation of intractable mature fibrils remains an enormous challenge. Encouraged by the above favorable outcomes, we further evaluated the reversal efficacy of PP[3]AS against aged fibrils. After incubation of insulin for 72 h and 144 h to produce varying degrees of fibration, PP[3]AS was immediately added. As shown in Fig. 5a, the absorbance of insulin decreased rapidly, ultimately reaching 95.36% and 92.17% dissolution of insulin fibrils. In addition, CD spectra showed that the ellipticities at two characteristic wavelengths were remarkably increased, indicating that PP[3]AS had the ability to disaggregate insulin fibrils, which was consistent with the absorbance result (Fig. 5b). Dissolution of the preformed insulin fibrils by PP[3]AS was also validated by TEM. Under treatment with PP[3]AS for 72 h, no appreciable pristine fibrils were observed (Fig. 5c and d). These results led us to believe that PP[3]AS possessed a reversal capability of insulin fibrillation both in the presence of "fibril seeds" or mature fibrils. Some representative inhibitors reported in the literature (macrocycles, polymers, peptides and small molecules) are listed in Table S1,† and by contrast, the present giant PP[3]AS displayed a superior anti-fibrillation capacity under conditions of both fibrillogenesis inhibition and fibril disintegration.

Prior to pharmacodynamics analysis, the biocompatibility of PP[3]AS was investigated *in vitro* and *in vivo*. The cytotoxicity on human normal renal epithelial cells (293T) and normal liver cells (LO2) was first evaluated by a Cell Counting Kit-8 (CCK-8) assay. As shown in Fig. 6a and S25,† PP[3]AS displayed minimal cytotoxicity against these two cell lines over the test range. Weight changes of mice after subcutaneous injection with a relatively high concentration of PP[3]AS (1000 μg kg^{-1}) were monitored to reflect systemic toxicity. PP[3]AS-treated mice had a body weight fluctuation similar to PBS-treated mice (Fig. 6b). On day 18 post administration, all the mice were euthanized and organ tissues and blood samples were harvested for the following analyses. The organ indexes of major organs, including heart, liver, spleen, lung, and kidney isolated from PP[3]AS-treated mice were comparable to those of mice treated with PBS, with no significant differences observed (Fig. 6c). The results of routine blood and blood chemistry assays revealed that representative hematological parameters of PP[3]AS-treated mice were comparable with those of mice in the PBS group

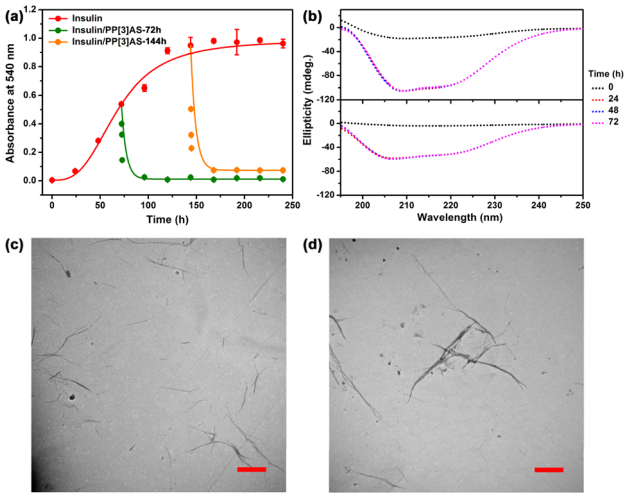

Fig. 5 (a) Disintegration of preformed insulin fibrils by PP[3]AS (344 μM), where the disintegrator was added to aggregating solution of 172 μM insulin at 72 and 144 h after initiation of aggregation. (b) Circular dichroism spectra of insulin (172 μM) in PBS buffer (10 mM, pH = 7.4) without or with application of PP[3]AS (344 μM) at different time points. PP[3]AS was added at 72 h (top) and 144 h (bottom) after initiation of aggregation. TEM images of insulin (172 μM) in PBS buffer (10 mM, pH = 7.4) with treatment of PP[3]AS (344 μM) for 72 h. PP[3]AS was added at (c) 72 h and (d) 144 h after initiation of aggregation.

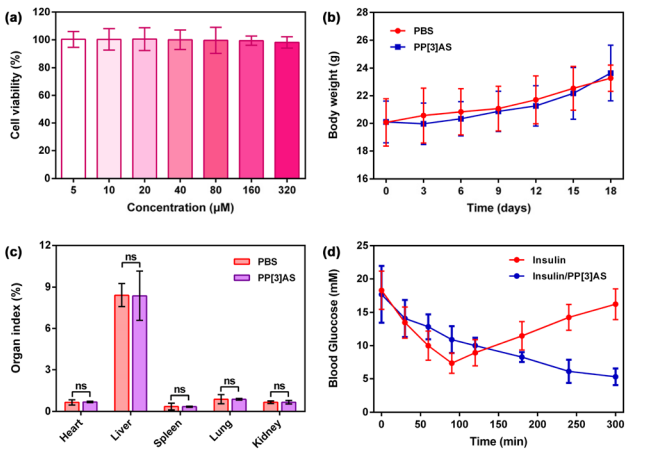

Fig. 6 (a) Relative cell viability of 293T cells treated with different concentrations of PP[3]AS for 24 h (mean ± S.D., $n = 5$). (b) Change in body weight of mice after subcutaneous injection with PP[3]AS compared with those injected with PBS ($n = 6$). (c) Major organ indexes of the mice on day 18 post-administration with PP[3]AS. Data are presented as mean ± S.D.; $n = 6$ for each group. The significance of difference was assessed using an unpaired *t*-test, ns: no significance. (d) Blood glucose concentration in STZ-induced diabetic mice after treatment with free insulin and insulin/PP[3]AS at predetermined intervals (mean ± S.D., $n = 6$). An unpaired *t*-test was performed at 300 min yielding significance ($P < 0.01$).

(Fig. S26 and S27†). Further support for low systemic toxicity is derived from histological analyses (Fig. S28†). Compared with the PBS group, no detectable inflammatory abnormalities or tissue damage could be observed in the PP[3]AS-treated group. Taken together, the above outcomes suggested that PP[3]AS could be safely applied in the following biological evaluation.

We then assessed the efficacy of insulin/PP[3]AS for the treatment of hyperglycemia in streptozotocin-induced diabetic mice (Fig. 6d). Following the onset of diabetes, mice were fasted for 6 h to ensure an average starting blood glucose level of ~11.1 mM. Recombinant insulin was then administrated subcutaneously at a dose of 100 μg kg^{-1}. Alternatively, an identical dose of insulin was administrated with PP[3]AS. Both insulin and insulin/PP[3]AS reduced the average blood glucose within 90 min. Subsequently, the mice that received free insulin became hyperglycemic again, whereas insulin/PP[3]AS-treated mice could remain normoglycemic until the 300 min endpoint of the study. Furthermore, the bioactivities of the disintegrated insulin fiber samples were also tested under the same experimental conditions. As shown in Fig. S29,† insulin with varying degrees of fibration after co-incubation with PP[3]AS for 12 h could exert a lower blood sugar effect to some extent. These favorable findings might be attributed to the known depot effect for insulin administration, in which the synthesized macrocycle could efficiently inhibit the formation of fibrillar aggregates. Excellent complexation strength and recognition selectivity embodied in insulin/PP[3]AS could be employed to avoid a burst release induced by blood thinning and competitive binding during the circulation process. The dynamic and reversible features of non-covalent interactions further endowed such a supramolecular formulation with sustained release of active insulin.

Conclusions

In conclusion, we successfully synthesized a novel pentaphen[3]arene sulfate with an interesting regulatory capacity for insulin aggregation. Not only could it inhibit the formation of amyloid, but also disaggregate intractable mature insulin fibrils. As compared with traditional macrocycles which recognize amino acid residues from the side, such macrocyclic inhibitors could achieve effective encapsulation of insulin at the C-terminal P11 sequence of the B chain. PP[3]AS exhibited robust binding affinities towards insulin with K_a values in the magnitude of 10^6 M^{-1}, and excellent anti-interference potency against various endogenous species. They also need to be aware that smaller CB[7] and CP5A cannot prevent insulin from fibrillation in the manner of local action. *In vitro* and *in vivo* safety evaluations proved initially that PP[3]AS possessed excellent biological compatibility. Co-administration with equimolar PP[3]AS could maintain normoglycemia for at least 5 h in streptozotocin-induced diabetic model mice, while mice treated with insulin alone became hyperglycemic again within 3 h. Potentially, this supramolecular strategy could be a versatile approach to regulating protein functions *via* host–guest interactions. Further studies exploring this possibility are ongoing in our laboratory.

Data availability

The data supporting this article have been included as part of the ESI.†

Author contributions

Designed research: R. W., J. C., Q. M., and C. L.; Performed research: R. W., Z. F., S. L., Z. Z., M. D., and J. C.; Analyzed data: R. W. and J. C.; Wrote the paper: R. W., J. C., and C. L.

Conflicts of interest

The authors declare no conflict of interest.

Acknowledgements

This work was financially supported by the National Natural Science Foundation of China (22171286 and 22201212), the Natural Science Foundation of Tianjin City (23JCZDJC00660), the Tianjin Municipal Education Commission (2021KJ188), and China Postdoctoral Science Foundation (2023M734309).

Notes and references

1 S. R. Pattan, P. Kekare, N. S. Dighe, S. A. Nirmal, D. S. Musmade, S. K. Parjane and A. V. Daithankar, *J. Chem. Pharm. Res.*, 2009, **1**, 191–198.
2 K. Suzuki, K. Hatzikotoulas, L. Southam, *et al.*, *Nature*, 2024, **627**, 347–357.
3 T. L. Blundell, J. F. Cutfield, G. G. Dodson, E. Dodson, D. C. Hodgkin and D. Mercola, *Biochem. J.*, 1971, **125**, 50P–51P.
4 L. Pirola, A. M. Johnston and E. V. Obberghen, *Diabetologia*, 2004, **47**, 170–184.
5 T. K. Mandal, *Am. J. Health-Syst. Pharm.*, 2005, **62**, 1359–1364.
6 J. Brange, L. Andersen, E. D. Laursen, G. Meyn and E. Rasmussen, *J. Pharm. Sci.*, 1997, **86**, 517–525.
7 Y. Hong, L. Meng, S. Chen, C. W. T. Leung, L. Da, M. Faisal, D. A. Silva, J. Liu, J. W. Y. Lam, X. Huang and B. Tang, *J. Am. Chem. Soc.*, 2012, **134**, 1680–1689.
8 D. Kerr, E. Wizemann, J. Senstius, M. Zacho and F. J. AmpudiaBlasco, *J. Diabetes Sci. Technol*, 2013, **7**, 1595–1606.
9 M. Groenning, S. Frokjaer and B. Vestergaard, *Curr. Protein Pept. Sci.*, 2009, **10**, 509–528.
10 M. Muzaffar and A. Ahmad, *PLoS One*, 2011, **6**, e27906.
11 J. Bieschke, J. Russ, R. P. Friedrich, D. E. Ehrnhoefer, H. Wobst, K. Neugebauer and E. E. Wanker, *Proc. Natl. Acad. Sci. U. S. A.*, 2010, **107**, 7710–7715.
12 N. Wang, J. He, A. Chang, Y. Wang, L. Xu, X. Chong, X. Lu, Y. Sun, X. Xia, H. Li, B. Zhang, Y. Song, A. Kato and G. W. Jones, *J. Agric. Food Chem.*, 2015, **63**, 1347–1351.
13 H. Wang, A. Li, M. Yang, Y. Zhao, L. Shi and R. Ma, *Sci. China:Chem.*, 2022, **65**, 353–362.
14 Y. Zhang, C. Li, X. Wu, F. Deng, F. Huang, Y. Zhang, J. Liu, H. Gui, R. Ma and L. Shi, *Chem. Eng. J.*, 2022, **435**, 134866.

15 H. Niu, X. Hou, Y. Zhang, X. Wu, F. Deng, F. Huang, L. Shi and R. Ma, *ACS Macro Lett.*, 2021, **10**, 662–670.
16 P. Yao, J. Zhang, S. You, W. Qi, R. Su and Z. He, *J. Mater. Chem. B*, 2020, **8**, 3076–3086.
17 K. L. Sciarretta, D. J. Gordon and S. C. Meredith, *Methods Enzymol.*, 2006, **413**, 273–312.
18 T. Takekiyo, E. Yamaguchi, H. Abe and Y. Yoshimura, *ACS Sustain. Chem. Eng.*, 2015, **4**, 422–428.
19 Z. Xu, S. Jia, W. Wang, Z. Yuan, B. J. Ravoo and D. S. Guo, *Nat. Chem.*, 2019, **11**, 86–93.
20 F. Biedermann and H. Schneider, *Chem. Rev.*, 2016, **116**, 5216–5300.
21 T. L. Mako, J. M. Racicot and M. Levine, *Chem. Rev.*, 2019, **119**, 322–477.
22 Y. Chen and Y. Liu, *Chem. Soc. Rev.*, 2010, **39**, 495–505.
23 M. J. Webber, E. A. Appel, B. Vinciguerra, A. B. Cortinas, L. S. Thapa, S. Jhunjhunwala, L. Isaacs, R. Langer and D. G. Anderson, *Proc. Natl. Acad. Sci.*, 2016, **113**, 14189–14194.
24 H. Zhao, X. Yang, Y. Pan, H. Tian, X. Hua and D. Guo, *Chin. Chem. Lett.*, 2020, **31**, 1873–1876.
25 K. Jie, Y. Zhou, E. Li and F. Huang, *Acc. Chem. Res.*, 2018, **51**, 2064–2072.
26 X. Ma and Y. Zhao, *Chem. Rev.*, 2015, **115**, 7794–7839.
27 A. Hennig, H. Bakirci and W. M. Nau, *Nat. Methods*, 2007, **4**, 629.
28 R. N. Dsouza, U. Pischel and W. M. Nau, *Chem. Rev.*, 2011, **111**, 7941–7980.
29 G. Ghale and W. M. Nau, *Acc. Chem. Res.*, 2014, **47**, 2150–2159.
30 M. S. Solum, C. L. Mayne, A. M. Orendt, R. J. Pugmire, J. Adams and T. H. Fletcher, *Energy Fuels*, 2014, **28**, 453–465.
31 X. Sun, A. Liu, K. Xu, Z. Zheng, K. Xu, M. Dong, B. Ding, J. Li, Z. Zhang and C. Li, *Aggregate*, 2024, e607.
32 Y. Zhao, L. Chen, J. Chen, J. Li, Q. Meng, A. Sue and C. Li, *Chem. Commun.*, 2023, **59**, 5858–5861.
33 H. C. Mahler, W. Friess, U. Grauschopf and S. Kieseet, *J. Pharm. Sci.*, 2009, **98**, 2909–2934.
34 H. C. Mahler, R. Muller, W. Friess, A. Delille and S. Matheus, *Eur. J. Pharm. Biopharm.*, 2005, **59**, 407–417.
35 J. W. Lee, M. H. Shin, W. Mobley, A. R. Urbach and H. I. Kim, *J. Am. Chem. Soc.*, 2015, **137**, 15322–15329.
36 L. Chen, Z. Meng, L. Tian, Y. Zhang, L. Zhao, X. Du, M. Ma, H. Zhang, J. Chen and Q. Meng, *Org. Biomol. Chem.*, 2022, **20**, 2222–2226.
37 M. Bouchard, J. Zurdo, E. J. Nettleton, C. M. Dobson and C. V. Robinson, *Protein Sci.*, 2000, **9**, 1960–1967.